

## LITERATURE CITED

1. I. A. Charnyi, Unsteady Motion of a Real Liquid in Pipes [in Russian], Nauka, Moscow (1975).
2. Kh. N. Nizamov, G. L. Batin, et al., "Promising methods of damping pressure oscillations in pipes," in: Hydroelastic Vibrations and Methods of Eliminating Them in Closed Piping Systems [in Russian], Krasnoyarsk (1983).
3. V. V. Berdnikov, T. S. Kozyreva, and B. A. Pantyukhin, "Study of the filling of a main line with liquid," Izv. Vyssh. Uchebn. Aviats. Tekh., No. 3 (1982).
4. T. Tomita and K. Nakamura, "Water hammer caused by air in a pump started with the discharge valve closed," Ebara Eng. Rev., No. 127 (1984).
5. A. Kitagawa, "A method of absorption for surge pressure in conduits," Bull. JSME, 22, No. 165 (1979).
6. S. P. Aktershev, A. V. Fedorov, and V. M. Fomin, "Mathematical modeling of tests of main pipelines for air-tightness with allowance for trapped volumes of air," in: Dynamics of Multiphase Media [in Russian], Novosibirsk (1985).
7. S. P. Aktershev, A. V. Fedorov, and V. M. Fomin, "Mathematical modeling of the filling of a main pipeline," in: Summary of Documents of the All-Union Seminar "Current Problems and Mathematical Methods of the Theory of Filtration," Moscow (1984).
8. A. A. Atavin and G. P. Skrebkov, "Simplified method of calculating pressure in a hydraulic system with a compensator," Vestn. Mashinostr., No. 8 (1962).
9. A. D. Al'tshul', Fluid Friction [in Russian], Nedra, Moscow (1982).
10. B. L. Rozhdestvenskii and N. N. Yanenko, Systems of Quasilinear Equations [in Russian], Nauka, Moscow (1978).
11. D. Contractor, "Use of transient regimes of fluid flow in the hydraulic excavation of mineral deposits," Trans. ASME, Teor. Osn. Inzh. Raschetov, No. 2 (1972).
12. A. Kitagawa, T. Takenaka, and Y. Kato, "Study of the high pressure generation by means of oil hammer," Bull. JSME, 27, 234 (1984).

NUMERICAL INVESTIGATION OF THE PROCESS OF SHOCK REFLECTION  
FROM A WALL WITH A SLOT HOLE

A. B. Britan, A. Ya. Rudnitskii,  
and A. M. Starik

UDC 533.6.07

The motion of shocks in channels of variable section is an important, hardly studied phenomenon that is utilized extensively in industrial technology, aerophysical experiment practice, and also in laboratory investigations utilizing shock tubes [1].

In the simplest case when two rectilinear channels of differing transverse dimensions are connected by a junction with a smooth change in section, analysis of the flow on both sides of the junction is ordinarily conducted within the framework of the quasistationary one-dimensional stream model [2-4]. In particular, for a channel with diminution of the cross-sectional area  $A$  quasistationary theory predicts four possible modifications of the flow wave structure, displayed schematically in the upper part of Fig. 1. Since the flow in the junction itself is not considered, the function is replaced by a discontinuity in the junction diagrams, at which the incident shock arrives from the left (the solid heavy lines are shock trajectories in space-time coordinates). The mode 1 with a reflected and passed shock between which the space is separated by a contact surface (its trajectory is shown by dashed lines in the diagrams) is realized for a subsonic stream velocity. As the incident shock intensity increases a nonstationary rarefaction wave (dash-dot) appears in the stream and accelerates the stream behind the passed wave to a supersonic velocity, mode 2. The reflected shock attenuates for small channel contractions and sufficiently high gas velocities, it ceases to move upstream, mode 3, and degenerates in the long run into a weak disturbance, mode 4 [2, 4]. The flow wave structure in mode 4 is determined by the passed shock and the rarefaction wave.

---

Moscow. Translated from Zhurnal Prikladnoi Mekhaniki i Tekhnicheskoi Fiziki, No. 6, pp. 112-118, November-December, 1987. Original article submitted July 28, 1986.

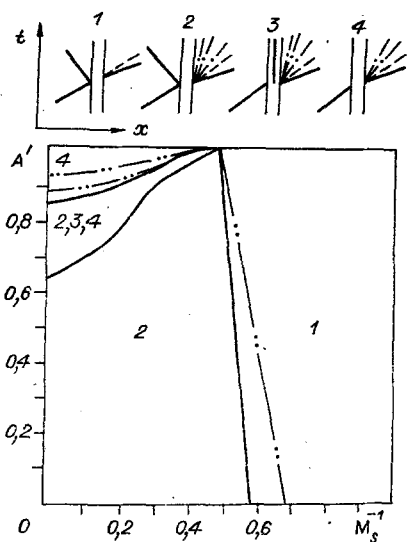


Fig. 1

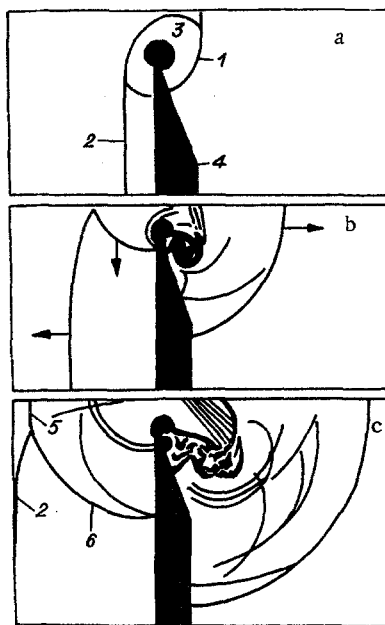


Fig. 2

The characteristic parameters on which the resultant wave structure depends are therefore the incident shock Mach number  $M_S = v_S/a_1$  ( $v_S$  and  $a_1$  are the incident shock velocity and the speed of sound in the unperturbed gas) and the relative channel dimension  $A' = A_1/A$  ( $A_1$  is the channel area in the exit section of the junction). The solid lines in Fig. 1 are the boundaries between the domains of values of the parameters  $M_S$  and  $A'$  for which the flow modes predicted by quasistationary theory for a perfect gas with adiabatic index  $\kappa = 1.4$  are realized. The numbering of the domains in the mode diagram and the wave structures in the upper part of Fig. 1 are in agreement.

An interesting feature of the mode diagram is the presence of domains in which three stationary wave structures 2, 3, 4 are possible (domain of coexistence). The problem of selecting the specific structure being realized in this part of the diagram for given  $M_S$  and  $A'$  was solved in [3] in conformity with the principle of minimum entropy production. However, it was later shown [5] that a unique solution without a reflected shock (mode 4) is realized in the coexistence domain, while the absence of a structure 3 was explained by the shock instability in the narrowing junction. This fact was recently confirmed in numerical computations [6] that also clarified the dynamics of flow development and the transition from mode 2 to mode 4. On the basis of the solution of the one-dimensional nonstationary gasdynamics equations for an inviscid, nonheat-conducting gas it has been obtained in [6] that the flow modes predicted by the quasistationary theory actually hold (with the exception of the features noted in the coexistence domain), where the time to shape the stationary stream depends substantially on the governing parameters of the problem  $M_S$  and  $A'$ .

It was noted above that a quasistationary analysis is applicable for flows sufficiently close to the one-dimensional, i.e., for channels connected by a junction with a moderate ( $\sim 10-15^\circ$ ) wall slope [6-8]. If channel contraction has the shape of a step or obstacle in the form of a reflecting wall with a hole, the flow pattern is complicated substantially [8-10].

Figure 2 shows a diagram of the flow restored by means of photographs of the shock reflection process from a wall whose right surface is cut at a  $20^\circ$  angle while the gap between the sharp edge and the upper wall of the channel forms a slot hole [10]. The incident shock arrives at the wall from the left and in the next instant (Fig. 2a) a rarefaction wave centered on the sharp edge of the reflecting wall 4 is present on shadow photographs together with the passed wave 1 and the planar part of the reflected front 2. Interaction between the rarefaction wave and the reflected shock front results in the formation of the curvilinear section of the front.

Further flow development is determined by interaction between the main elements of the pattern themselves and with the channel walls. The photograph in Fig. 2b is obtained at a later time when a Mach configuration is formed because of shock reflection; the arrows indicate the directions of main perturbation motion. Clearly seen in Fig. 2c is the rectilinear

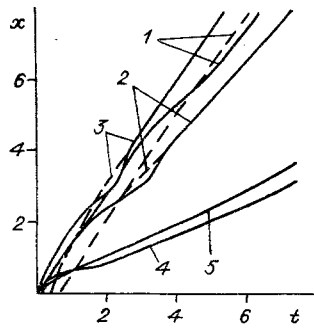


Fig. 3

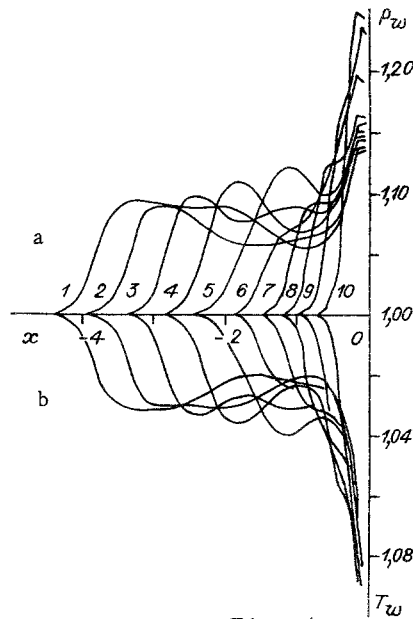


Fig. 4

shock 5 of the Mach configuration, the Mach stem, the reflected front section 2 and the curvilinear shock 6 occupying a significant stream domain to the left of the reflecting wall up to now. The complex flow to the right of the wall is governed by diffraction of the passed wave in the expanding channel [11, 12] as well as by viscous effects in the stream and vortex formation in the neighborhood of the sharp edge. Not only the nonstationary but also the substantially two-dimensional nature of the stream should be taken into account to analyze the flow pattern on both sides of the reflecting wall. It can be assumed in advance (in particular, this is mentioned in [4]) that the two-dimensional effects change even the resultant flow structure, which will be different, for given  $M_S$  and  $A'$ , from the mode predicted by the quasistationary stream model. Since there are no appropriate computations, it is of interest to perform a numerical modeling of the process and to study the influence of the governing parameters on the resultant flow pattern upon shock reflection from a wall with a slot hole.

A plane channel of height  $2H$  with endface wall in the section  $x = 0$  at which a plane incident shock front arrives from the left at the time  $t = 0$ , was considered in the computations. There is a slot hole in the wall whose height is  $2h$  from the sharp edge, and goes over into the expanding nozzle for  $x > 0$ . The gas on the right of the incident shock front is at rest. Numerical integration of the two-dimensional nonstationary equations describing the inviscid and non-heat conducting perfect gas flow was executed by the Godunov method [13] in the Kolgan [14] modification to assure second-order accuracy in the space coordinates and first-order accuracy in the time.

Nonpenetration conditions were imposed on the solid impermeable walls, and the condition of "nonreflection" of the perturbations on the right and left boundaries of the computation domain [13]. It was assumed that the gas parameters on the left boundary correspond to conditions behind the incident shock (pressure  $p = p_2$ , density  $\rho = \rho_2$ , longitudinal velocity component  $u = u_2$ , transverse component  $v = 0$ ), and conditions in the unperturbed gas on the right boundary ( $p_1, \rho_1, u_1 = v_1 = 0$ ).

Taken as the initial distribution was  $p = p_2, \rho = \rho_2, a = a_2, u = u_2, v = 0$  for  $x \leq 0$  and  $p = p_1, \rho = \rho_1, a = a_1, u = 0, v = 0$  for  $x > 0$ . Dimensionless variables were used with the previous notation retained, where half the slot height  $h$ , the sound speed  $a_1$ , and the density  $\rho_1$  were the length, velocity, and density scales. The scales for the pressure, time, and temperature were  $\rho_1 a_1^2, h/a_1$ , and  $a_1^2/R$  ( $R$  is the gas constant). The computation (for  $x < 0$ ) was performed on a rectangular mesh without explicit separation of the discontinuities. The extent of the computation domain along the  $Ox$  axis occupied not more than  $13h$ , out of which the length of the section to the left of the wall ( $x < 0$ ) was  $9h$  while the maximal number of computational cells reaches 6500.

An anomalous pressure surge on the endface wall was observed in the computations at the initial time but it vanished sufficiently rapidly. Moreover, formation of an entropy layer

that was conserved throughout the extent of the computation was noted near the wall. Such "effects" were not taken into account in the flow pattern analysis since they are associated with features of the numerical method and do not affect the results of the computations.

Before going over to an analysis of the results obtained, we consider certain regularities of the development of the reflection pattern with time. Detailed processing and classification of numerous shadow photographs of the stream, performed in [9], showed that two phases exist for the process of plane reflected shock front formation. The first phase of duration  $t_1$  is governed by the interaction between the curvilinear shocks 6 and is terminated by the formation of a Mach configuration (see Fig. 2b and c) and the Mach stem on the channel axis. The second phase is accompanied by growth of the Mach stem, which increases to dimensions of the height  $H$  in the time  $t_2$ .

The main result of the experiments [9] is establishment of a self-similar nature of the wave processes accompanying the reflected shock formation in agreement with the deductions of [10], it should be emphasized here that only the location and dimensions of the main flow pattern elements at different times were determined in both researches. In practice there are no data on the influence of the processes mentioned on the gas stagnation parameters in the area of the channel endface wall in the literature. The set of values of  $t_1$  and  $t_2$ , obtained in different experimental conditions, is presented in [9] without discussion of the specific dependence of these characteristics on the governing parameters  $M_s$  and  $A'$ .

The results of the numerical investigation show that  $t_1$  depends mainly on local effects in the area of the hole whose relative dimension  $A'$  exerts no influence on the process in the initial stage since the channel side walls take no part in it. As noted in [9], the sound speed  $a_2$  can be a characteristic quantity governing the rate of formation of conditions in the area of the hole for  $t < t_1$ . As  $M_s$  increases the values of  $t_1$  and  $t_2$  are shortened, where  $t_2$  also depends on the parameter  $A'$  since the time during which the triple point of the Mach configuration reaches the channel side wall grows as the absolute size of the hole diminishes.

A change in the growth rate of the Mach stem associated with features of the process development at the time when the curvilinear shock 6 of the Mach configuration goes over from the endface to the side wall of the channel, is detected in the computations. Further process of the shock 6 occurs as the velocity grows until the configuration triple point reaches the side wall, where this effect is later manifest as the parameters  $M_s$  and  $A'$  diminish. According to the computations under the conditions of the experiment [10], deviation of the process from self-similarity should set in 160-170 msec after formation of the Mach configuration, however, the observation time in [10] is considerably smaller (~100 msec), consequently, the mentioned effect is not recorded in the experiments.

The non-self-similar nature of the processes accompanying the reflected shock front formation is also manifest in the behavior of the motion trajectories of the axial and near-wall parts of the front.

Presented in Fig. 3 are the appropriate trajectories in space-time coordinates as computed for several values of  $M_s$  and  $A'$ . The solid curves correspond to the channel axis, and the dashes to the side wall. Trajectories for  $M_s = 4, 4, 6, 6, 8$  and  $A' = 0.162, 0.333, 0.333, 0.8, 0.8$  are shown by numbers 1-5. Intersection of the curves with the  $t$  axis corresponds to the time of curvilinear shock reflection from the channel axis (see Fig. 2b). By virtue of the reasons discussed above, the time  $t \leq t_1$  is independent of  $A'$  and diminishes as  $M_s$  grows.

A remarkable feature of all the curves is the presence of a section on which the near-axis part of the reflected front overtakes the near-wall section, therefore, the front starts to be bent towards the side opposite to the channel reflecting wall. Computations show that in this stage of formation of the reflected shock front, the curvilinear shock 6 of the Mach configuration moves from the channel side wall to the axis. The Mach stem occupies a whole section of the channel, however, the stream parameters continue to depend on the interaction processes of the main wave structure elements.

Certain details of the formulation of the pressure  $p_w$  and temperature  $T_w$  distributions at the side wall illustrate the computation results in Fig. 4. The case of subsonic flow behind the incident shock ( $M_s = 1.52$ ) for a large size hole  $A' = 0.91$  was considered, the numbers 1-10 correspond to the times  $t = 7.5, 6.5, 5.5, 4.5, 3.5, 2.5, 1.75, 1.25, 0.8, 0.4$ .

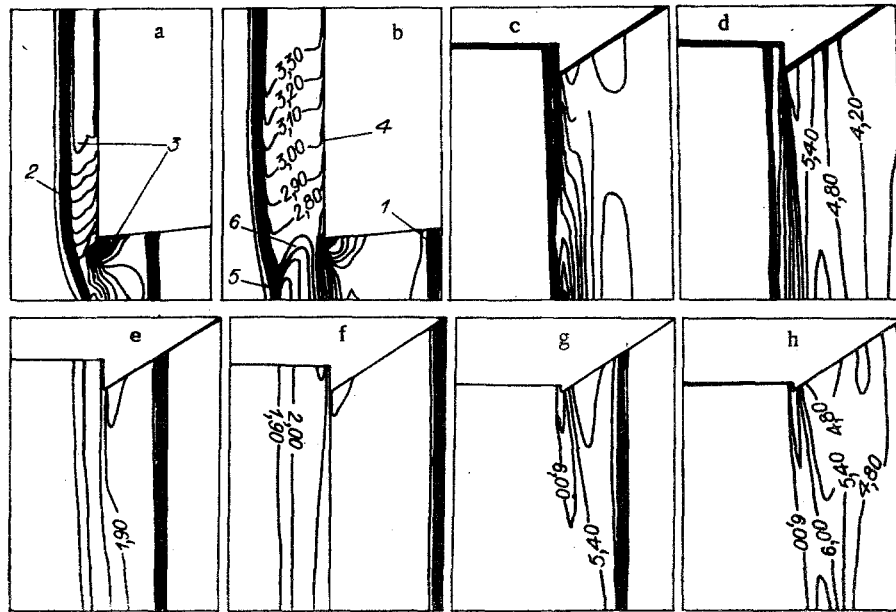


Fig. 5

The distance between the hole edges and the channel side wall is small in this case and the influence of the hole is felt continuously on the behavior of the stagnation parameters. Successive reflections of the rarefaction wave and the curvilinear shock from the wall result in fluctuations of the parameters throughout the whole computation time. A domain of elevated values of the temperature and pressure, which is related to stream stagnation in angular domains and in which conditions close to the flow behind a detached compression shock are realized, is formed near the reflecting wall ( $x \sim 0.5$ ). Elevation of the parameters in the entropy layer (as already mentioned; it is not shown in Fig. 4) is usually localized in a sufficiently narrow zone ( $x < 0.15$ ) adjoining the endface and is not more than 3-4% of the values of  $p_w$  and  $T_w$ . The parameters on the side wall gradually approach the stationary values, however, the behavior of the pressure and temperature indicates a substantially two-dimensional nature of the processes behind a reflected shock for a significant time ( $t \sim 6.5$ ). Utilization of the quasistationary theory (see, e.g., [15]) results in this case in substantial errors in the determination of the stream parameters. Let us note for comparison with Fig. 4 that under these conditions the quasistationary theory yields  $p_w = 1.011$ ,  $T_w = 1.003$  while the parameters  $p_w = 2.2$ ,  $T_w = 1.28$  are realized for reflection of a shock from a "blank" wall.

It is interesting to compare configurations occurring in a two-dimensional stream during shock reflection from a wall with a hole to the wave structures 1-4 (see Fig. 1). Such a comparison is especially urgent for large relative hole dimensions since both computational and experimental results are substantially absent in the upper domain of the mode diagram which would permit restoration of the flow pattern under conditions of substantial influence of the two-dimensional effects.

Figure 5 shows the computed distributions of the constant density lines (isopycn) in a stream, obtained for different reflection conditions. The isopycns in Fig. 5a and b correspond to a channel geometry and shock intensity in experiments [10] ( $M_s = 1.52$ ,  $A' = 0.167$ ). The main elements of the Mach shock configuration, the passed wave, and the rarefaction wave are reliably separated in the numerical modeling (the perturbation notations in Figs. 2 and 5 agree). Up to the time  $t = 1.25$  and  $2.5$  (Fig. 5a and b), the computed flow pattern to the left of the wall endface agrees with the shadow photographs in Fig. 2a and b. A wave structure characteristic for the mode 1 is shaped, however, a nonstationary rarefaction wave associated with channel broadening for  $x > 0$  appears to the right of the hole. As  $A'$  increases to  $0.91$  for  $M_s = 1.52$  the rarefaction wave vanishes (Fig. 5e and f) and mode 1 with a subsonic velocity in the whole flow domain between the reflected and passed shocks is built up. The computation shows that the influence of a large hole attenuates the reflected shock, the individual stages of stationary pattern formation here seems to be compressed in time (see also Fig. 3, curves 3 and 4). In contrast to Fig. 5b there is no curvilinear shock 6 in Fig. 5f up to the time  $t = 2.5$ , and the reflected shock front is sufficiently rectilinear. The

gas parameters on the side wall change in conformity with the data in Fig. 4 while the reflected wave trajectories on the channel axis and wall agree in practice. This is precisely why dashed lines are not presented for curves 4 and 5 in Fig. 3.

For  $M_w \geq 2.1$  the flow is reconstructed according to the wave structure of mode 2, which is conserved up to  $A' \leq 0.80$ . As the hole increases further, attenuation of the reflected shock results in the formation of a stationary configuration with a shock localized in the neighborhood of the section  $x = 0$ . Starting with  $A' = 0.91$ , the reflection pattern recalls the mode 3 predicated by quasistationary theory which would be conserved in the whole range of  $M_s$  variation. The fact of the existence of such a configuration for  $A' = 0.91$  would have been difficult to assume beforehand since the endface wall in this case is substantially replaced by a small step at the channel side wall. The isopycn distribution in the stream is presented in Fig. 5c and d for the times  $t = 1.25$  and 4, respectively, for the mode mentioned ( $M_s = 4$ ,  $A' = 0.91$ ). Despite the significant hole dimensions, clearly traced in the initial stages of the reflection (Fig. 5c) is the process of Mach stem formation on the channel axis and the curvilinear shock interacts downstream with the noticeably deformed rarefaction wave.

The stationary pattern of isopycn distribution is displayed in Fig. 5d, from which it is seen that the reflected shock front is rectilinear and transposed upstream. An increase in the incident shock  $M_s$  for  $A' = 0.91$  does not result in spoilage of the reflection pattern but only changes the coordinate of the stationary location of the reflected shock. For  $M_s = 8$  the reflected shock was twice as close to the section  $x = 0$  than for  $M_s = 4$ , and as  $A'$  diminished started to move upstream in conformity with the wave structure of mode 2. Let us also note that no domain of mode coexistence predicted by the quasistationary theory (see Fig. 1) was detected in the computations.

The boundaries between the corresponding domains of values of  $M_s$  and  $A'$ , computed in the two-dimensional formulation, are presented in Fig. 1 by dashes with two dots. Shifting of the boundaries between modes 1 and 2 shows that for an abrupt contraction of the channel a supersonic flow is set up behind the passed shock for lower values of  $M_s$  than in the one-dimensional stream. The location of this boundary depends substantially on the channel geometry downstream of the endface wall also. Results of the computation in Fig. 1 are obtained for a channel with parallel walls for  $x > 0$ . If the channel expanded for  $x > 0$  (see Fig. 5), the stream behind the passed wave can become supersonic even when  $u_2 < a_2$  behind the incident shock. In particular, this latter means that mode 1 is realized in the domain of values of  $M_s$  and  $A'$  corresponding just to the right upper part of the mode diagram in Fig. 1 (for  $A' > 0.7$ ) in the reflecting nozzles of shock tubes. The sequence of reflection pattern formation for  $A' = 0.91$ ,  $M_s = 1.52$  can be tracked from the data in Fig. 4 and Fig. 5e and f.

The two-dimensional nature of the reflection process results in a shift of the boundaries even in the left part of the mode diagram. The lower dash-dot boundary separates the domain of parameter values for modes 2 and 3, where mode 3 is realized in the two-dimensional stream in a sufficiently narrow range of variation of the relative hole dimensions. For  $A' > 0.91$  a mode of supersonic flow around an obstacle is formulated (a parameter domain above the upper dash-dot curve), which the computed isopycns presented in Fig. 5g and h for  $M_s = 8$  and  $A' = 0.97$  and the times  $t = 0.2$  and 1.75, respectively, demonstrate.

The oblique compression shock is seen in Fig. 5g, which still does not reach the channel axis, the nonstationary rarefaction fan at the sharp edge of the hole, and the passed shock to the right of the hole. The pattern recalls the early stage of flow formation in other modes (see Fig. 5a, say), however, in this case the process seems "frozen" and the shock interaction on the axis does not later go over into Mach interaction. Let us note that the horizontal scale of the figures is 4.13 times coarser than the vertical, consequently all the isopycns appear somewhat compressed in the longitudinal direction and the slopes of the perturbations differ from the actual ones. The oblique shock with density drop  $\rho/\rho_2 = 6$  in Fig. 5h is reflected from the channel axis and its shape and slope to the stream are governed by the transverse distribution of the local  $M_2$ . For the conditions considered ( $M_s = 8$ ), on the stream axis  $M_2 = 1.79$  while the slope of the shock is close to  $45^\circ$ . The possibility of the existence of such a mode for large values of  $A'$  was discussed in [9]; let us note also that in the considered range of variation of  $M_s$  and  $A'$  no condition for the origination of the mode 4 was detected.

In channels with abrupt narrowing of the area the flow mode around a sharp step with an oblique compression shock is realized for  $M_s > 2$  and small step size (~7% of the channel

area). In the mentioned range of parameters the rounding off of the sharp step should result in the appearance of a mode 4 and the influence of the step on the parameters in the stream core should thereby be diminished.

The authors are grateful to V. A. Levin for constructive remarks during discussions of the results of the research.

#### LITERATURE CITED

1. T. V. Bazhenova and L. G. Gvozdeva, Nonstationary Shock Interaction [in Russian], Nauka (1977).
2. A. K. Oppenheim, P. A. Urtiew, and A. J. Laderman, "Vector polar method for the evaluation of wave interaction processes," Arch. Budowy Mash., 11, No. 13 (1964).
3. A. K. Oppenheim, P. A. Urtiew, and R. A. Stern, "Peculiarity of shock impingement on area convergence," Phys. Fluids, 2, No. 4 (1959).
4. W. Chester, "The propagation of shock waves along ducts of varying cross section," Adv. Appl. Mech., 6, 119 (1960).
5. G. Rudinger, "Passage of shock waves through ducts of variable cross section," Phys. Fluids, 3, No. 3 (1960).
6. D. R. Greatrix and J. J. Gottlib, "An analytical and numerical study of a shock wave interaction with an area change," UTIAS Report No. 268 (1982).
7. V. L. Grigorenko, "Numerical investigation of the shock triggering of supersonic nozzles and comparison with experimental data," Izv. Akad. Nauk SSSR, Mekh. Zhidk. Gaza, No. 1 (1980).
8. G. A. Bird, "The effect of wall shape on the degree of reinforcement of a shock wave moving into a converging channel," J. Fluid Mech., 5, No. 1 (1959).
9. G. N. Nikolaev, "Experimental investigation of the formation of a shock wave reflected from a wall with a hole," Izv. Akad. Nauk SSSR, Mekh. Zhidk. Gaza, No. 2 (1974).
10. G. Chardin, "Example of shock tube application to the solution of nonstationary gas-dynamics problems," in: Shock Tubes [Russian translation], IL, Moscow (1962).
11. V. T. Grin', A. N. Kraiko, and N. N. Slavyanov, "Solution of the problem of triggering a nozzle mounted in the endface of a shock tube," Izv. Akad. Nauk SSSR, Mekh. Zhidk. Gaza, No. 6 (1981).
12. A. B. Britan and E. I. Vasil'ev, "Singularities of flow formation in a profiled nozzle of a shock tube," Dokl. Akad. Nauk SSSR, 281, No. 2 (1985).
13. S. K. Godunov, A. V. Zabrodin, M. Ya. Ivanov, et al., Numerical Solution of Multidimensional Gasdynamics Problems [in Russian], Nauka, Moscow (1976).
14. V. P. Kolgan, "Application of the principle of the minimal value of the derivative to the construction of finite-difference schemes to compute discontinuous solutions of the gasdynamics equations," Uchen. Zap., TsAGI, 3, No. 6 (1972).
15. V. Ya. Bezmenov and V. V. Osipov, "Influence of the critical nozzle section area of a wind tunnel on gas flow in a channel," Uchen. Zap. TsAGI, 12, No. 6 (1981).